

# INVESTIGATION OF TECHNOLOGICAL EFFECTS OF BALL BURNISHING AFTER CRYOGENIC TURNING OF HARD STEEL

Krzysztof Żak, Wit Grzesik

## Summary

This paper presents investigations of a sequential machining process which incorporates CBN hard turning with cryogenic pre-cooling of the workpiece (CHT) and ball burnishing (BB). The main goal of this study was to select machining conditions enhancing the quality of parts machined by hard turning including the surface roughness  $R_a$  of about  $0.2 \mu\text{m}$ , good bearing properties and reducing the white layer. The obtained technological effects were characterized in terms of surface roughness, surface texture, microstructure alterations and micro-hardness distribution.

**Keywords:** cryogenic hard turning, ball burnishing, surface texture, hardened alloy steel

## Badanie efektów technologicznych nagniatania tocznego kulką po kriogenicznym toczeniu stali utwardzonej

### Streszczenie

Przedstawione w pracy wyniki badań doświadczalnych sekwencyjnego procesu obróbki obejmują toczenie utwardzonej stali 41Cr4 chłodzonej kriogenicznie narzędziem z CBN i nagniatanie kulką. Podstawowym celem badań był dobór warunków obróbki, zwiększających jakość elementów toczonych na twardo z uwzględnieniem kryterium chropowatości powierzchni  $R_a$  (ok.  $0.2 \mu\text{m}$ ), dobrej nośności powierzchni i ograniczenie białej warstwy. Ocena uzyskanych efektów technologicznych wykonano na podstawie chropowatości powierzchni, cech tekstury powierzchni, zmian morfologii mikrostruktury warstwy wierzchniej i rozkładu twardości.

**Słowa kluczowe:** kriogeniczne toczenie na twardo, nagniatanie kulką, stal utwardzona, struktura geometryczna powierzchni

## 1. Introduction

Modern machining processes need to be more and more effective, less costly, environmental friendly and sustainable. These criteria are often applied to hard and cryogenic machining operations as references. In general, machining of hardened steels was proven to be an effective and economically efficient removal technology in many top-level manufacturing branches including

---

Address: Prof. Wit GRZESIK, Krzysztof ŻAK, PhD, Opole University of Technology, Faculty of Mechanical Engineering, Mikołajczyka 5, 45-271 Opole, Poland. Phone: (+48, 77) 4498461, Fax: (+48, 77) 4499927, e-mail: w.grzesik@po.opole.pl, k.zak@po.opole.pl

automotive, bearing, hydraulic and die and mold making sectors [1, 2]. However, hard machining is not capable to replace grinding operations as predicted a few decades ago despite many technological advantages [2-4]. As a result, a new idea to integrate these finishing processes has been elaborated but it requires the stiff machine tools with good damping to minimize the cutting vibrations [4]. In practice, hard turned parts are obviously finished with special abrasive operations, such as finishing grinding, superfinishing, belt grinding and honing or mass finishing [5]. Relatively new technology which is capable of limiting these technological bottlenecks is sliding or roller burnishing of the hard turned or milled surfaces. Special commercial tooling, as for instance, hydrostatic burnishing heads are applied on CNC machine tools along with conventional cutting tools with one tool magazine.

Incidentally, roller and sliding burnishing of steels, aluminium alloys, titanium and its alloys, as well as other non-ferrous materials, with a surface hardness up to 50 HRC has been successfully applied in the industry for a few decades. At present, burnishing is developed for light and heat resistant aerospace materials using CNC 5-axes machining centers. Burnishing of a bearing steel of 62 HRC hardness causes that the  $R_a$  parameter is reduced below  $0.2 \mu\text{m}$  and due to the reduction of cutting temperature, the high compressive residual stresses of  $-1600 \text{ MPa}$  are induced into the surface sublayer [6].

The characteristic index expressed by the ratio of  $R_{a_t}/R_{a_b}$  ( $R_{a_t}$  and  $R_{a_b}$  are values  $R_a$  roughness parameter after turning and burnishing respectively) ranges from 1.4 to 2.4 [7]. It was achieved after burnishing a hardened steel component (64 HRC) with the pressure of 38 MPa using a ceramic ball of 6.35 mm diameter. As previously, surface roughness  $R_{a_b}$  decreased to about  $R_a = 0.2 \mu\text{m}$ . Practically the same surface effect was obtained in this study but in a different technological process.

On the other hand, sustainable cryogenic machining is extensively applied for machining of many advanced engineering materials (structural ceramics, titanium alloys, HRSA's) to reduce the cutting temperature, tool wear and process stability. In the case of hardened steels it is used to eliminate structural alterations, especially white layer formation [8, 9]. It has been reported by Umbrello [10] that cryogenic turning of AISI 52100 bearing steel results in substantial reduction of the white layer thickness from  $4 \mu\text{m}$  during dry cutting to less than  $1 \mu\text{m}$ . Moreover, it decreases with reduction of the initial hardness of the machined steel from 61 HRC to 54 HRC. This fact inspired authors to investigate deeply the effects of cryogenic treatment of the workpiece before ball burnishing. The preliminary assessment of technological effects resulting from ball burnishing of dry hard turned surfaces was reported by authors in Refs. [11-13]. This study is focused on a sequential machining process which aggregates hard machining of cryogenically pre-cooled bearing steel and ball burnishing. In other words it incorporates the synergic effects of cryogenic treatment and deformation of surface irregularities by the hard burnishing element.

## 2. Experimental studies

### 2.1. Machining conditions

In this study low alloyed 41Cr4 (AISI 5140) steel with Rockwell's hardness of  $57\pm 1$  HRC was machined using TNGA 160408 S01030 chamfered CBN inserts, grade CB7015 by SandvikCoromant. The sample was cryogenically pre-cooled in a special chamber with liquid nitrogen (LN2) [14]. A characteristic ice skin which covered the workpiece after cryogenic freezing is seen in Fig. 1a. Hard turning conditions were selected as follows: cutting speed of 150 m/min, three feed rates of 0.075 (CHT1), 0.1 (CHT2) and 0.125 (CHT3) mm/rev, depth of cut of 0.15 mm/rev. It allows initially turned surfaces with different values of the Ra parameter to be further flattened and hardened by ball burnishing.

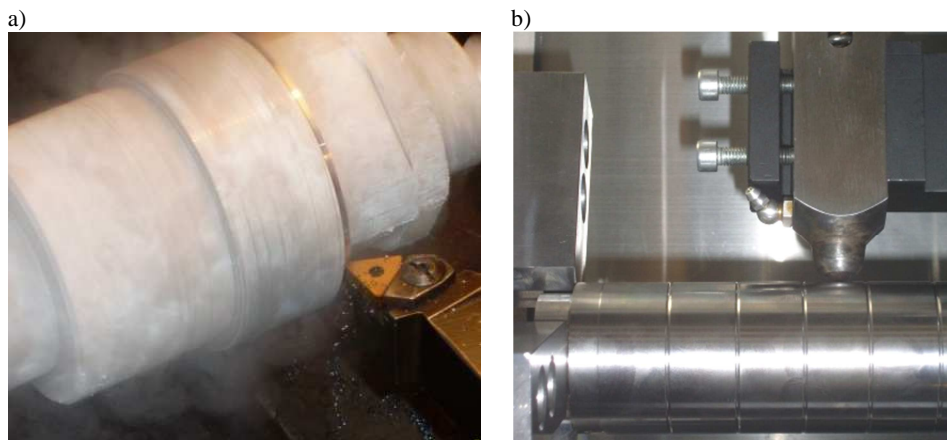


Fig. 1. Cryogenic hard turning with CBN tool (a) and ball burnishing with  $\text{Si}_3\text{N}_4$  ball (b) operations

Roller burnishing operations were performed on a CNC turning center, Okuma Genos L200E-M, using special burnishing tool equipped with  $\text{Si}_3\text{N}_4$  ceramic ball of 12 mm diameter shown in Fig. 1b. The desired load of about 60 N was generated by controlled spring-based pressure system. It was realized by the tool correction of 0.25 mm in the CNC control system. Burnishing conditions were selected as follows: burnishing speed of 25 m/min, burnishing feed  $f_b$  of 0.05 (BB1), 0.075 (BB2) and 0.1 (BB3) mm/rev.

### 2.2. Measurements of surface and subsurface characteristics

Surface profiles/ topographies were recorded using a TOPO-01P contact profilometer with a diamond stylus radius of  $2\ \mu\text{m}$ . After their digitalization, 2D and 3D roughness parameters were estimated on the selected scanned areas of

2.4 mm × 2.4 mm. Micro-hardness  $HV_{0.05}$  of the as-machined and polished samples across the subsurface was measured using a LECO Vickers hardness tester MHT Series 200 with a Berkovich indenter. In each case, a micro-hardness distribution at the distance of 100 μm from the machined surface was determined. In order to avoid interference of neighboring indentations and increase the measuring accuracy, the measurements were performed on the cross-sections, inclined at about 3° to the outer surface (see Fig. 10a). Based on the micro-hardness recordings, the strain-hardening rates related to the maximum values of microhardness in the subsurface layer were computed.

The microstructure and texture changes induced by burnishing were examined by means of a scanning microscope, model HITACHI S-3400N equipped with an X-ray diffraction head EDS, model THOMO NORAN System Six. Both SEM and BSE images were recorded. These analyses were performed on mechanically and chemically polished sections.

### 3. Results and discussion

#### 3.1. Height and amplitude of surface roughness parameters

The effects of the ball burnishing of initially turned pre-cooled surfaces based on characterization of their geometrical features are shown in Figs. 2-6 and in Table 1.

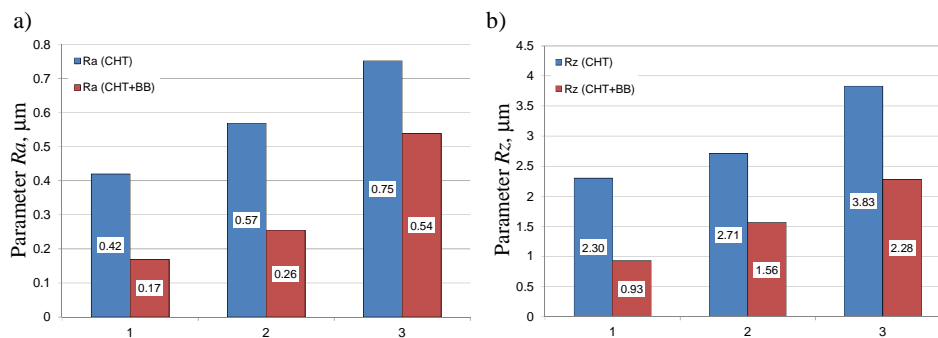


Fig. 2. Comparison of  $R_a$  and  $R_z$  roughness parameters for hard turned and ball burnished surfaces, 1 –  $f_i = 0.075$  mm/rev, 2 –  $f_i = 0.1$  mm/rev, 3 –  $f_i = 0.125$  mm/rev

Figure 2 presents the measured values of the  $R_a$  and  $R_z$  parameters and their reduction due to burnishing action for different feeds. In general, for sequential (CHT+BB) operations the index  $R_{at}/R_{ab}$  decreases from 2.47 to about 1.39 when the feed rate increases. This indicates that burnishing diminishes the  $R_a$  parameter but its reduction below 0.2 μm was obtained for variant 1 (CHT1+BB1) with a minimum feed rate. In this case the minimum value of

$R_a = 0.17 \mu\text{m}$  was obtained. Moreover, cryogenic HT produced profiles with higher peaks disturbed by the side flow effect [3] and burnishing is able to modify turned profiles effectively rather at smaller feeds. This effect results from increased hardness and strenght as well as coarser microstructure of the freezing workpiece [9].

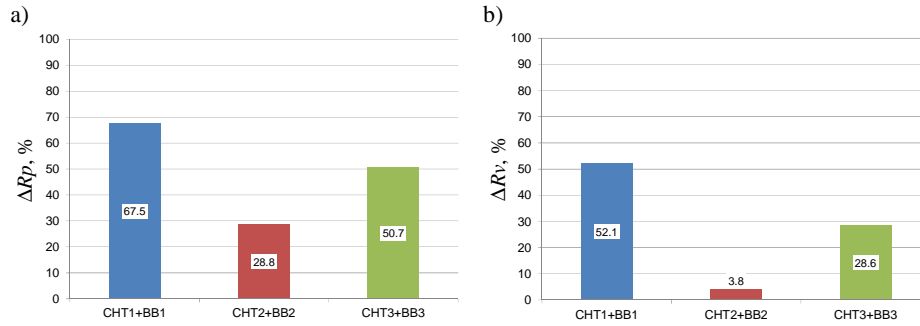


Fig. 3. Percentage changes of  $R_p$  (a) and  $R_v$  (b) components of the maximum profile height  $R_z$

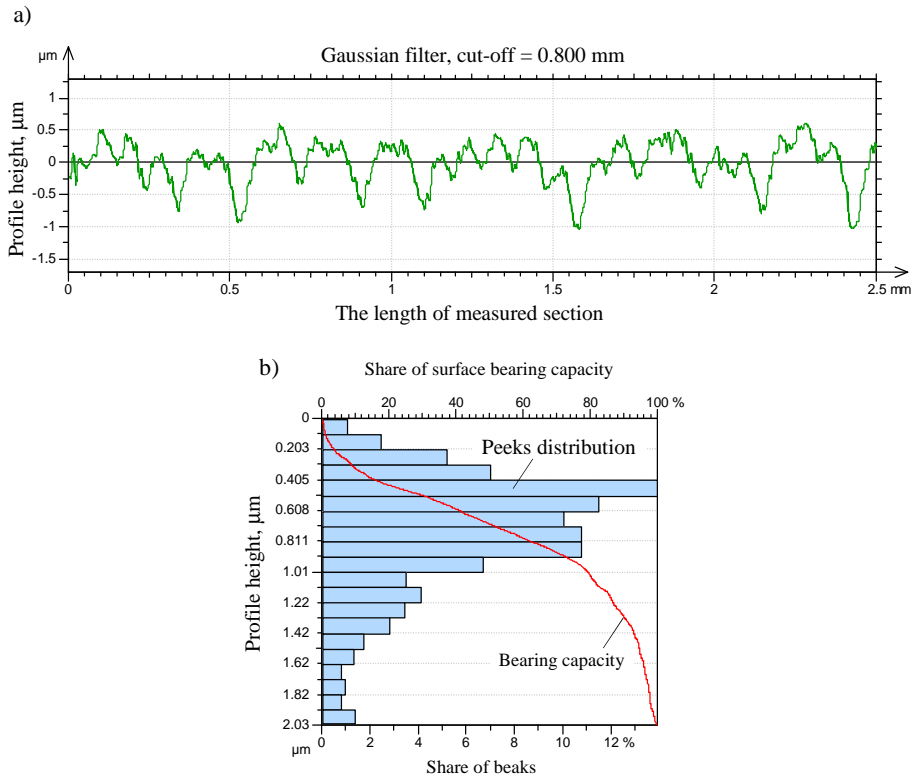


Fig. 4. Exemplary surface profile (a) and associated BAC histogram (b) for CHT2+BB2

For instance, for subsequent operation CHT2+BB2 the peaks were reduced by 28.8% and the valleys only by 3.8%. This comparison suggests that peaks are partly fractured because plastic deformations of brittle material is substantially limited (only about 29% as mentioned above). As shown in Fig. 4a burnishing produces a plateau-type of the surface profile with the bearing area curve (BAC) shown in Fig. 4b. In this case the shape of the amplitude distribution function (ADF) is asymmetric and extremely shifted towards the peaks [13].

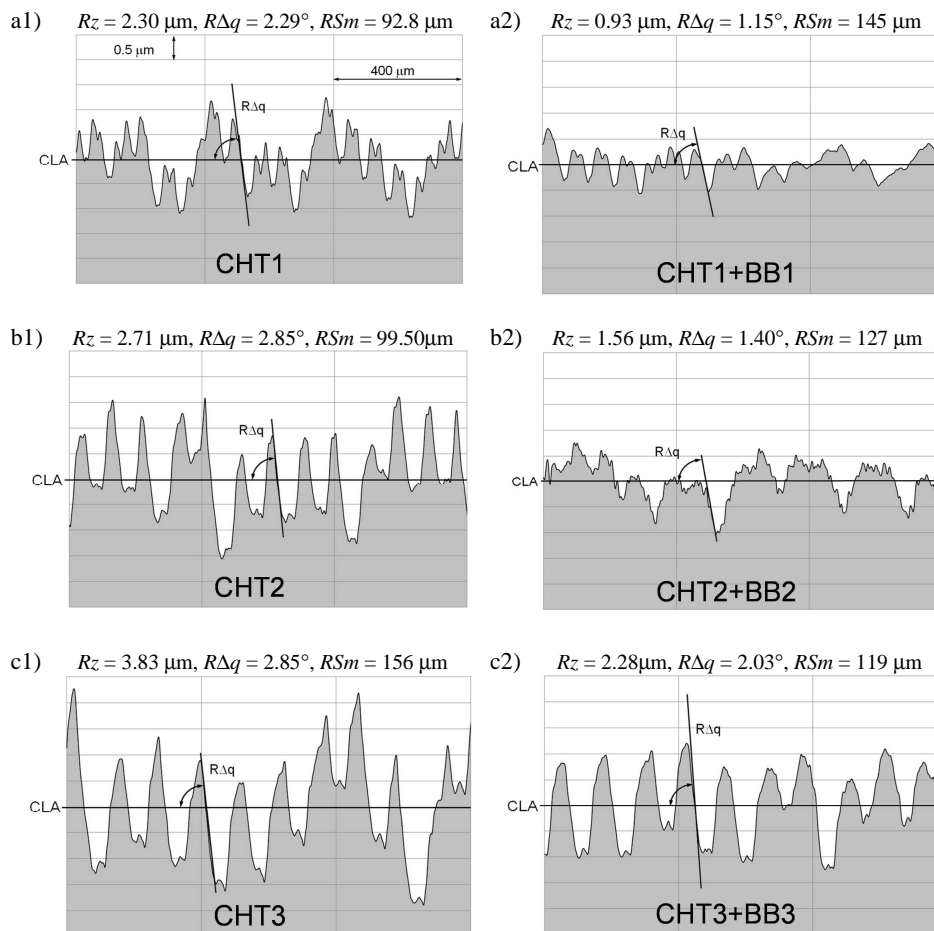


Fig. 5. Modifications of surface profiles produced in cryogenic (a1-c1) hard turning by ball burnishing operations (a2-c2)

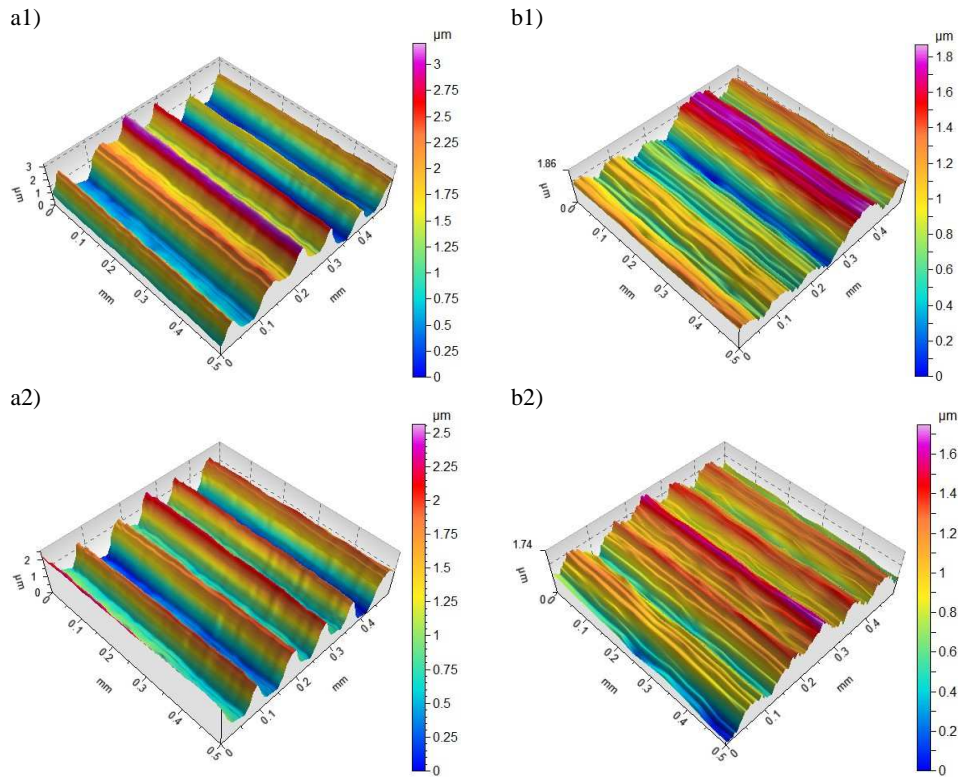


Fig. 6. Surface topographies produced in cryogenic hard turning (a) and by ball burnishing operations (b) (corresponding surface profiles as in Fig. 5)

Table 1. Values of 2D surface roughness parameters after CHT and subsequent BB operations

| SR parameters<br>$\mu\text{m}$ | Cryogenic hard turning |       |       | Sequential operations |          |          |
|--------------------------------|------------------------|-------|-------|-----------------------|----------|----------|
|                                | CHT1                   | CHT2  | CHT3  | CHT1+BB1              | CHT2+BB2 | CHT3+BB3 |
| $Ra$                           | 0.42                   | 0.57  | 0.75  | 0.17                  | 0.26     | 0.54     |
| $Rz$                           | 2.30                   | 2.71  | 3.83  | 0.93                  | 1.56     | 2.28     |
| $Rp$                           | 1.11                   | 1.50  | 2.05  | 0.36                  | 0.57     | 1.01     |
| $Rv$                           | 1.19                   | 1.21  | 1.78  | 0.57                  | 0.99     | 1.27     |
| $RSm$                          | 92.8                   | 99.5  | 156   | 145                   | 127.00   | 120      |
| $Rku$                          | 2.57                   | 2.15  | 2.31  | 3.22                  | 3.64     | 1.99     |
| $Rsk$                          | -0.14                  | 0.26  | -0.03 | -0.72                 | -0.96    | -0.47    |
| $Rdq$                          | 2.29                   | 2.85  | 2.74  | 1.15                  | 1.40     | 2.03     |
| $Rpk$                          | 0.155                  | 0.503 | 0.658 | 0.210                 | 0.0671   | 0.163    |

The second observation is that changes of  $Rp$  and  $Rv$  component within the total height  $Rz$  depend on the initial profile shape. Figure 3 shows percentage changes of  $Rp$  and  $Rv$  roughness parameters which constitute the entire surface

profile ( $R_z = R_p + R_v$ ). For fine profile produced with smaller turning and burnishing feeds changes of  $R_p$  and  $R_v$  components are quite proportional (67.5% vs. 52.1%). On the other hand, burnishing profile with substantially higher peaks (higher  $R_z$  parameter) results in larger deformations of peaks in comparison to reduction of valleys ( $R_v$ ).

Figure 5 presents some zoomed fragments of surface profiles produced by hard turning and ball burnishing. As can be seen in Fig. 5 cryogenic hard turning produced surface profiles with non-regular tool nose traces, for which the  $R_{sm}$  parameter is higher than feed value, with very small slopes  $R\Delta q$ , generally in the range of 2-3°. For the case of CHT1+BB1/BB2, burnishing deforms sharp peaks within  $R_p$  height and also changes the  $R_{sm}$  parameter. Moreover, profile slope  $R\Delta q$  decreases by 1.2-2.0° depending on the burnishing feed. Otherwise, for the case of CHT3+BB3 during which higher irregularities are partly spalled and severely deformed, and finally flattened, new modified profile with lower spacing between peaks is produced. For this effect,  $R_{sm}$  decreases about 20% (see Figs. 5c1 vs. c2).

Some representative fragments of surface topographies are shown in Fig. 6. In this case the zooming technique was the same as for surface profiles presented in Fig. 5. Because the profile contains asperities with different heights burnishing can produce textures with differently deformed profiles, as shown in Fig. 6b1 and b2. As a result, generated textures contain more or less fragments of uniformly deformed asperities ( Fig. 6b1 vs. 6b2).

### 3.2. Bearing properties

Figure 7 confirms that CBN hard turning of cryogenically pre-cooled parts produces profiles with unsatisfactory bearing properties and additional roller burnishing operations enhance them depending on initial cutting parameters. In general, this effect is not so distinct as for dry hard turning with the same feed rates [11]. However, burnishing of surfaces generated in cryogenic HT causes that new surfaces profiles with negative skewness and kurtosis between 2 and 3.5 (Fig. 8a) are produced. The surface profile presented in Fig. 4 is the case when  $R_{ku} > 3$  and  $R_{sk} < 0$ .

It should be noted in Fig. 8b that correspondingly to bearing curves # 4-6 shown in Fig. 7, negative values of the skewness  $R_{sk} = -0.72, -0.96$  and  $-0.47$  were determined respectively. In the case study the largest effect was obtained for the variant CHT2+BB2 for which  $R_{sk} = -0.96$ . The final surface profile for this case of sequential machining is shown in Fig. 4a. Corresponding BAC has characteristic  $S$  (progressive-degressive) shape (curve # 5 in Fig. 7). From this point of view, the burnishing effect of  $R_a$  below 0.3  $\mu\text{m}$  needs the original turned surface profiles with the  $R_z$  parameter not higher than 3  $\mu\text{m}$ .

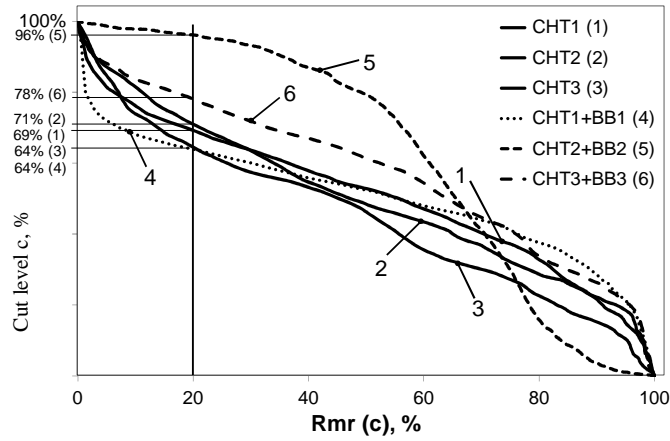


Fig. 7. Material ratio curves for hard turning (CHT) and sequential (CHT+BB) operations

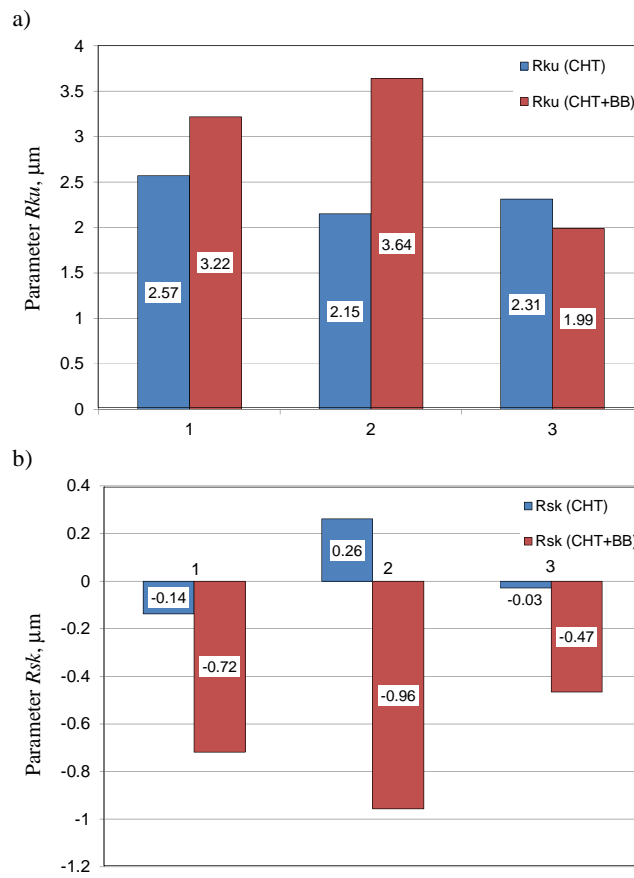


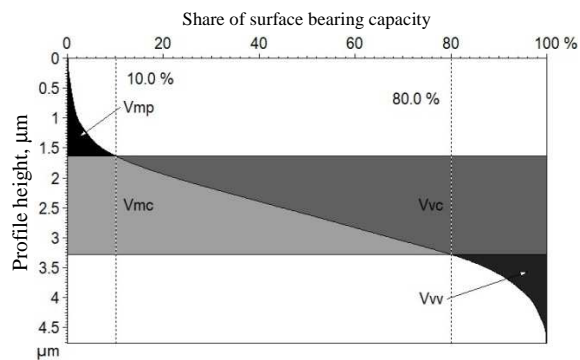
Fig. 8. Kurtosis (a) and skewness (b) distributions for a range of sequential operations

Moreover, burnishing causes reduction of the  $Rpk$  parameter, which defines the material part removed during the running-in period. It allows reducing  $Rpk$  by several times, from 0.50 to 0.07  $\mu\text{m}$  for (CHT+BB) with the feed ratio of  $f_t/f_b = 0.1/0.075$  mm/rev.

### 3.3. Area height distribution parameters

The functional parameters which characterize bearing and oil retention properties include the surface bearing index ( $Sbi$ ), the core fluid retention index ( $Sci$ ) and the valley fluid retention index ( $Svi$ ). The value of  $Sbi = 0.58$  for burnished surface indicates lower wear of peaks (shorter running-in period). On the other hand, the large value of  $Sci = 1.53$  suggests good fluid retention of the turned surface. Moreover, larger value of  $Svi = 0.140$  for the burnished surface

- a) CHT2 ( $V_{mp} = 0.0389$  ml/m<sup>2</sup>,  $V_{vc} = 0.936$  ml/m<sup>2</sup>,  
 $V_{mc} = 0.711$  ml/m<sup>2</sup>,  $V_{vv} = 0.0824$  ml/m<sup>2</sup>)



- b) CHT2+BB2 ( $V_{mp} = 0.0169$  ml/m<sup>2</sup>,  $V_{vc} = 0.479$  ml/m<sup>2</sup>,  
 $V_{mc} = 0.350$  ml/m<sup>2</sup>,  $V_{vv} = 0.0579$  ml/m<sup>2</sup>)

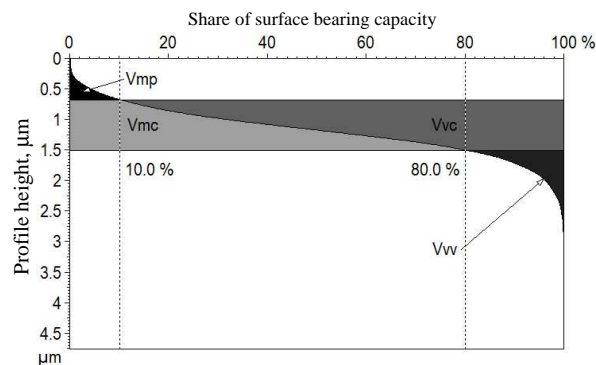


Fig. 9. Volume functional parameters for cryogenic hard turning CHT2 (a) and burnishing (b) operations

indicates a good fluid retention ability in the valley zone. The volume functional parameters, which are based on the 3D BAC, include the material volume of the surface ( $S_m$  or  $V_m$ ), the core void volume ( $S_c$  or  $V_{vc}$ ) and the valley void volume ( $S_v$  or  $V_{vv}$ ) parameters. At first glance, these parameters represent volumes equivalent of the  $S_{bi}$ ,  $S_{ci}$  and  $S_{vi}$  and their interpretations have the same meanings.

Their distributions and values obtained for CHT and BB operations are presented in Fig. 9.

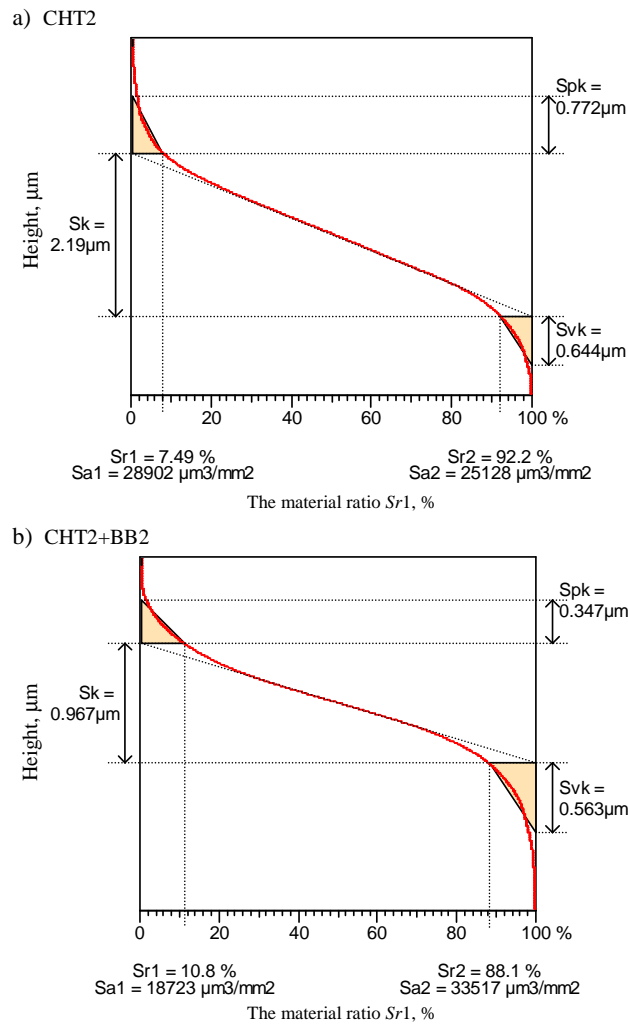


Fig. 10. Comparison of 3D BAC parameters for hard turning (a) and sequential (b) processes

3D bearing ratio parameters include the areal material ratio ( $S_{mr}$ ) and the inverse areal material ratio ( $S_{mc}$ ). The interpretation of the areal material ratio ( $S_{mr}$ ) is that its higher value indicates better bearing and wear properties. In this aspect, distinctly higher value of  $S_{mr} = 31.9\%$  determined for burnished surfaces re-confirms their good bearing properties in comparison to hard turned surfaces for which  $S_{mr} = 2.0\%$ .

The inverse areal material ratio ( $S_{mc}$ ) defines the height which ensures the specified material ratio  $S_{mr}$ . In the sequential process its value is reduced from 0.98 and to 0.52  $\mu\text{m}$ . Moreover, the material ratio  $S_{r1} = 10.8\%$  for the burnished surface was determined at the height of 0.347  $\mu\text{m}$ , but for highly peaked turned surface the  $S_{r1} = 7.49\%$  was obtained at the height of 0.772  $\mu\text{m}$ , as shown in Fig. 10.

### 3.4. Area spatial and hybrid parameters

The values of four 3D spatial parameters are specified in Table 2. The burnished surfaces contain distinctly more summits within the scanned area –  $S_{ds} = 1996 \text{ 1/mm}^2$  versus  $593 \text{ 1/mm}^2$  for turned surfaces. The texture aspect ratio  $S_{tr}$  is higher for burnished surfaces but its values for both operations less than 0.1 are characteristic for highly anisotropic surfaces [14]. The texture direction  $S_{td}$  close to  $90^\circ$  indicates that the dominant surface lay is perpendicular to the measurement direction. The values of  $S_{al}$  parameter (the fastest decay autocorrelation length) obtained suggest that the burnished texture is more dominated by long wavelength unit events, whereas the turned texture is dominated by short wavelength feed-marks.

Table 2. Values of 3D (area) spatial parameters

| Parameter                | CHT2   | CHT2+BB2 |
|--------------------------|--------|----------|
| $S_{ds}, \text{ 1/mm}^2$ | 593    | 1996     |
| $S_{tr}, \text{ mm}$     | 0.0309 | 0.085    |
| $S_{td}, ^\circ$         | 89.8   | 90.0     |
| $S_{al}, \text{ mm}$     | 0.0374 | 0.103    |

The values of three 3D hybrid parameters are specified in Table 3. The burnished surfaces contain irregularities with lower slopes  $S_{dq}$  – about  $2.6^\circ$  versus  $4.2^\circ$  for turned surfaces. This comparison coincides with 2D slope data presented in Fig. 5. The values of the average summit curvature  $S_{sc}$  of about  $0.007 \mu\text{m}^{-1}$  agree with those for typical machined surfaces ( $0.004\text{-}0.03 \mu\text{m}^{-1}$ ) given in [14]. The  $S_{dr}$  parameter (the developed interfacial area ration) is higher for turned surfaces for which the smallest unit of plane area is about 0.09 %. On the other hand, the burnished surface (Fig. 6b1 and b2) contains very small

irregularities within the single peaks and, in turn,  $Sdr$  is smaller (0.035%) than for the turned surface.

Table 3. Values of 3D (area) hybrid parameters

| Parameter             | CHT2       | CHT2+BB2   |
|-----------------------|------------|------------|
| $Sdq$                 | 0.0423     | 0.0264     |
| $Ssc, 1/mm (1/\mu m)$ | 6.63/0.007 | 7.23/0.007 |
| $Sdr, \%$             | 0.0893     | 0.0349     |

### 3.5. Micro-hardness distribution and strain-hardening effect

Typical measuring problem which influences measuring accuracy is that interferences of indentations can occur across the subsurface layer of dozens of microns. To minimize this effect and to increase the measuring accuracy ( $h_i = l_i \times \sin \alpha$ ), the measurements were performed on the sections, inclined at the angle  $\alpha \approx 3^\circ$  to the outer surface as shown in Fig. 11a. Sample was mounted in conductive resin and gradually finished by mechanical grinding, diamond polishing and electropolishing.

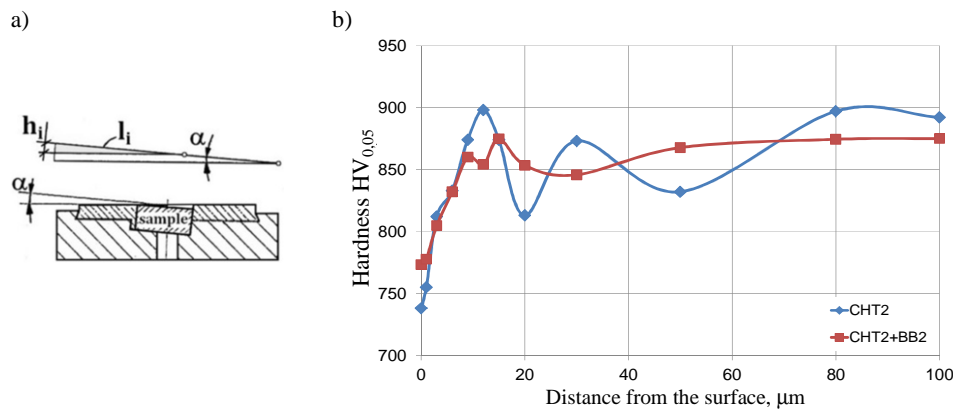


Fig. 11. Preparation of inclined sections for micro-indentation Vickers tests (a) and micro-hardness distributions for cryogenic hard turning and sequential operations (b). Feed ratio:  $f_t/f_b = 0.1/0.075$  mm/rev

The distribution of micro-hardness in the subsurface layer at the distance of 100  $\mu m$  from the surface before and after burnishing is shown in Fig. 11b. It is evident in Fig. 11b that for cryogenic cooling the maximum micro-hardness is shifted beneath the surface (12-15  $\mu m$  in depth).

As a result, Vickers micro-hardness in the zone adjacent to the surface is about 740 MPa and increases slightly to 775 MPa after burnishing. This fact suggests that after cryogenic hard turning (CHT2) white layer is not produced. On the other hand, it suggests only superficial effects resulting from ball action during burnishing.

When comparing the hardening coefficients  $S_h$  ( $S_h = (\mu\text{HV}_b - \mu\text{HV}_i)/\mu\text{HV}_i$ ) related to the maximum values of  $\text{HV}_{0.05}$  obtained for hard turning and sequential HT-B operations its value increases from about 5% to 10% depending on the process variant. This is due to the fact that the austenite reach WL (about 60% austenite [1]) is more extensively hardened than martensite structure obtained in CHT. The strain-hardening effect due to burnishing can be explained in terms of the austenite-martensite phase transformation, during which the surface layer has practically martensite structure without retained austenite after burnishing.

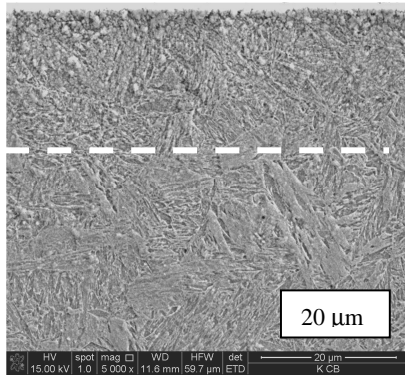
### 3.6. Microstructure and chemical composition

In this study, quantitative microstructure analysis was performed using SEM/BSE technique with additional phase content measurements using EDS technique. The second technique allows the chemical composition of the surface layer to be determined and the structural effect of burnishing operations to be identified.

BSE analysis of the bulk material after hard dry machining confirms characteristic microstructure consisting of martensite and retained austenite [11]. On the other hand, cryogenic machining reduces the amount of retained austenite which agrees with observations in Ref. [10]. Fig. 12 shows BSE microphotographs of surface layer (SL) produced by cryogenic hard turning (Fig. 12a) as well its modifications induced by sequential burnishing (Fig. 12b) respectively. It should be noted that the width of the surface layer (maximum 20  $\mu\text{m}$ ) coincides well with microhardness distribution presented in Fig. 11b. Moreover, the thickness of DSL in Fig. 12 agrees, in percentage, with the effects of plastic deformation and reduction of  $S_z$  parameter (4.76 vs. 2.84  $\mu\text{m}$ ) due to burnishing. Again, it confirms the occurrence of brittle fractures of surface peaks. The BSE images confirm that LIN pre-cooling of the workpiece causes that the white layer (WL) is not produced, whereas for dry HT its width is about 10  $\mu\text{m}$  [12]. On the other hand, LIN machining produced a significantly coarser structure with submicron carbides.

EDS spectrum presented in Fig. 13 suggests no evidence of a chemical modification within the subsurface layer. This observation coincides with conclusion given in Ref. [6]. Only some marginal inclusions of silicon were detected, probably transferred from the ball surface due to its abrasive wear during matting with extremely hard steel.

a) finer martensite microstructure in SL



b) smaller thickness of deformed SL

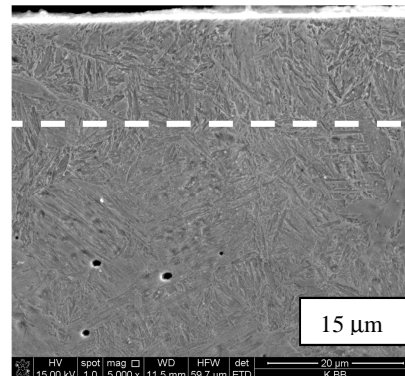


Fig. 12. Microstructures of the surface layer (SL) after: (a) cryogenic hard machining (CHT2) and (b) sequential CHT2+BB2 [11]. Magnification $\times$  5000

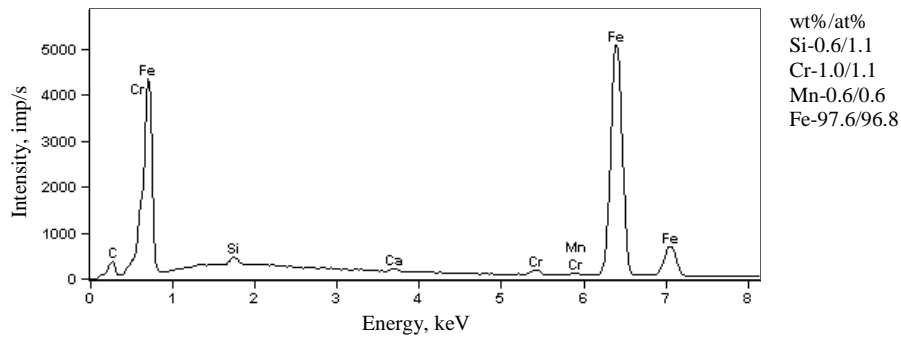


Fig. 13. EDS spectrum of the surface layer after sequential CHT2+BB2 process

#### 4. Conclusions

The following practical findings resulted from this study:

1) Ball burnishing of turned surfaces of pre-cooled steel parts modifies both surface texture and subsurface layer. In particular, white layer formation is diminished.

2) Turned surfaces are flattened due to burnishing. This effect is higher for smaller initial roughness. Surfaces with  $R_a$  parameter below  $0.2 \mu\text{m}$ ,  $R_z$  parameter lower than  $1 \mu\text{m}$  and  $Rpk$  parameter of about  $0.1 \mu\text{m}$  can be generated.

3) Better bearing properties of burnished surfaces are documented by higher negative values of skewness  $Rsk$ . Also functional indices are visibly favourable.

4) The strain-hardening due to additional burnishing is in the range of 5%, which suggests brittle fracture of sharp peaks. Higher microhardness readings above 850 HV were obtained at the distance lower than 20  $\mu\text{m}$  from the surface.

5) Hardening of the surface layer after ball burnishing is caused by transformation of austenite into martensite. This observation coincides with the mechanism documented by Umbrello [10].

### References

- [1] G. BYRNE, D. DORNFELD, B. DENKENA: Advancing cutting technology. *Annals of the CIRP*, **52**(2003)2, 483-507.
- [2] F. KLOCKE, BRINKSMEIER, K. WEINERT: Capability profile of hard cutting and grinding processes. *Annals of the CIRP*, **54**(2005)2, 557-580.
- [3] W. GRZESIK: *Advanced Machining Processes of Metallic Materials*. Elsevier, Amsterdam 2008.
- [4] JP. DAVIM (ed.): *Machining of Hard Materials*, Springer, London 2011.
- [5] W. GRZESIK, J. RECH, T. WANAT: Surface finish on hardened bearing steel parts produced by superhard and abrasive tools. *Inter. Journal of Machine Tools and Manufacture*, **47**(2007), 255-262.
- [6] F. KLOCKE, J. LIERMAN: Roller burnishing of hard turned surfaces. *Inter. Journal of Machine Tools and Manufacture*, **38**(1998), 419-423.
- [7] L. LUCA, S. NEAGU-VENTZEL, I. MARINESCU: Effects of working parameters on surface finish in ball-burnishing of hardened steels. *Precision Engineering*, **29**(2005), 253-256.
- [8] F. PUŠAVEC, E. GOVEKAR, J. KOPAČ: Jawahir IS The Influence of Cryogenic Cooling on Process Stability in Turning Operations. *CIRP Annals-Manufacturing Technology*, **60**(2011)1, 101-104.
- [9] Y. YILDIZ, M. NALBANT: A Review of cryogenic cooling in machining processes. *Inter. Journal of Machine Tools and Manufacture*, **48**(2008), 947-964.
- [10] D. UMBRELLO: Analysis of the white layer formed during machining of hardened AISI 52100 steel under dry and cryogenic cooling conditions. *Inter. Journal of Advanced Manufacturing Technology*, **64**(2013), 633-642.
- [11] W. GRZESIK, K. ŻAK: Producing high quality parts using sequential hard turning and ball burnishing operations. *Precision Engineering*, **37**(2013), 849-855.
- [12] W. GRZESIK, K. ŻAK: Modification of surface finish produced by hard turning using superfinishing and burnishing operations. *Journal of Materials Processing Technology*, **212**(2012), 315-322.
- [13] W. GRZESIK: Functional properties of hardened steel parts generated by turning and ball burnishing operations. *Advances in Manufacturing Science and Technology*, **36**(2012)4, 5-17.
- [14] B. GRIFFITHS: *Manufacturing Surface Technology. Surface Integrity and Functional Performance*. Penton Press, London 2001.

Received in October 2013